Marine Micropaleontology 125 (2016) 36–50

Contents lists available at ScienceDirect

Marine Micropaleontology

journal homepage: www.elsevier.com/locate/marmicro

Deciphering processes controlling mid-Jurassic coccolith turnover

Fabienne Giraud [a,b,*], Emanuela Mattioli [c], Gatsby Emperatriz López-Otálvaro [c,d], Christophe Lécuyer [c,1], Baptiste Suchéras-Marx [e], Yves Alméras [f], François Martineau [c], Florent Arnaud-Godet [c], Eric de Kænel [g]

[a] Université Grenoble Alpes, ISTerre, F-38041 Grenoble, France
[b] CNRS, ISTerre, F-38041 Grenoble, France
[c] Univ Lyon, Université Claude Bernard Lyon 1, Ens de Lyon, CNRS, UMR 5276 LGL-TPE, F-69622 Villeurbanne, France
[d] Department of Geology, University of Salamanca, 37008 Salamanca, Spain
[e] Aix-Marseille Université, CNRS, IRD, CEREGE UM34, 13545 Aix en Provence, France
[f] 29 Impasse des Mésanges, 01700 Beynost, France
[g] DPR, Matile 51, 2000, Neuchatel, Switzerland

ARTICLE INFO

Article history:
Received 5 August 2015
Received in revised form 4 March 2016
Accepted 8 March 2016
Available online 10 March 2016

Keywords:
Aalenian–Bajocian
Lotharingius
Watznaueria
Coccolithophore evolution
Brachiopod
Geochemistry
Paleoceanography

ABSTRACT

The Middle Jurassic is characterized by major changes within the fossil coccolithophorid community, with a transition from *Lotharingius*-dominated to *Watznaueria*-dominated assemblages, concomitant with a significant increase in the pelagic carbonate production. The mechanisms that triggered this overturn remain poorly understood. Here, we present a compilation (new and previously published data) of *Lotharingius* and *Watznaueria* abundances through the Early–Middle Jurassic transition. Alongside this, trends in newly-acquired and literature-derived carbon and oxygen isotope data were used to represent paleoceanographic indicators, such as nutrient and temperature changes. The nannofossil data show a rapid (around 1.5 Myr) turnover around the Aalenian–Bajocian transition. Across the Aalenian/Bajocian boundary, assemblages dominated by *Lotharingius* spp. give way to assemblages dominated by *Watznaueria* spp., coinciding with a peak in a particular morphological group of *Watznaueria* (species with a cross in the central area). The proliferation of this morphogroup occurred during a time of oceanic opening and rearrangement of ocean circulation. This led on to the evolution of pioneering coccolithophorid taxa, but also to extinctions in several marine groups. In the Early Bajocian, the proliferation of two other morphogroups (*Watznaueria* without a central-area structure and *Watznaueria* with a bar) corresponds to the major diversification of *Watznaueria*, and the beginning of its Mesozoic dominance. The *Watznaueria* diversification and dominance are associated with radiation in other marine groups, and these biotic changes occurred during a time of putative enhanced oceanic fertility and relatively low temperatures. This study suggests that restructuring of fossil coccolithophorid communities may be favored during short turnover intervals related to major paleoceanographic change.

1. Introduction

During the Mesozoic Era, the Middle Jurassic was a key period for plankton evolution in marine environments, probably related to the opening of large oceanic domains, such as the Alpine Tethys and the central Atlantic Ocean. Nannofossil plankton carbonate production increased at that time and contributed significantly to the pelagic carbonate sedimentation in open oceans (Suchéras-Marx et al., 2012, 2014). The most remarkable pattern in nannofossil assemblages identified during this time is the transition between the coccolith genera *Lotharingius*, dominant in the Toarcian (Cobianchi, 1992; Cobianchi et al., 1992; Mattioli and Erba, 1999) and *Watznaueria*, which was dominant from the Middle Jurassic to the end of the Early Cretaceous, and ubiquitous in Upper Cretaceous assemblages (Erba, 1990; Lees et al., 2005; Linnert and Mutterlose, 2009; Tiraboschi and Erba, 2010). The transition between these two genera is well known and well defined in terms of phyletic relationships (Bown, 1987; Cobianchi et al., 1992; Mattioli, 1996). However, abundance changes precisely documenting this transition across the Early–Middle Jurassic transition are generally limited to semi-quantitative data, published as distribution charts for the western Tethys (Erba, 1990; Cobianchi et al., 1992; Reale et al., 1992; Stoico and Baldanza, 1995; Fauconnier et al., 1996; Chiari et al., 2007; Sandoval et al., 2008; Tiraboschi and Erba, 2010), and there is no up-to-date assessment of these data, nor any report on the quantitative abundance changes through time. We present in this study the abundance data for *Lotharingius* and *Watznaueria* through the Early–Middle Jurassic transition using new and published data. Correlation of these data

* Corresponding author at: Université Grenoble Alpes, ISTerre, F-38041 Grenoble, France.
E-mail address: Fabienne.Giraud-Guillot@ujf-grenoble.fr (F. Giraud).
[1] Institut Universitaire de France.

http://dx.doi.org/10.1016/j.marmicro.2016.03.001
0377-8398/

with external proxies for paleoenvironmental change has allowed us to conjecture on which processes, biotic or abiotic, triggered this significant shift.

Sea-surface temperatures and surface-water nutrient levels are the two major parameters controlling nannoplankton distribution and proliferation (McIntyre et al., 1970; Okada and Honjo, 1973; Balch, 2004). In the geological record, these two parameters can be reconstructed, to some extent, using stable oxygen and carbon isotope data. For the Jurassic, several data, coming from both Tethyan and boreal regions, are available. These carbon and oxygen isotope data were measured on different fossil remains, such as bivalve shells (Paris Basin: France, Brigaud et al., 2009); and belemnite rostra (Lusitanian Basin: Portugal, Jenkyns et al., 2002; Basque–Cantabrian Basin: northeastern Spain, Gomez et al., 2009). Carbon and oxygen isotope ratios have also been

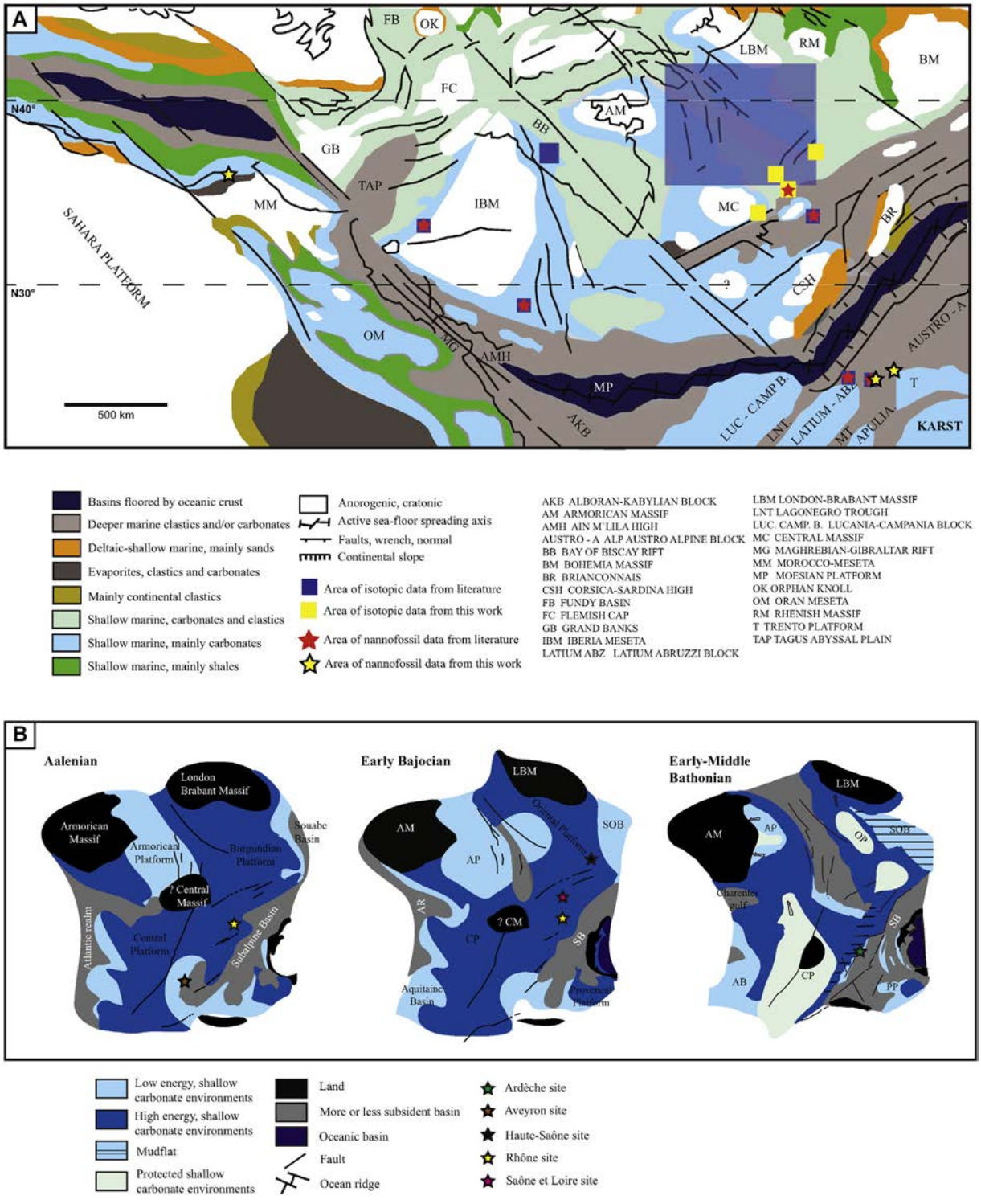

Fig. 1. A. Paleogeography of the western Tethys during the Bajocian–Bathonian interval, re-drawn after Ziegler (1988), showing sample locations. B. Three detailed paleogeographic maps from the Aalenian to the Middle Bathonian, redrawn after Enay and Mangold (1980), showing both the location and the paleoenvironments of selected brachiopod samples for carbon and oxygen isotope analyses. Abbreviations: AB: Aquitaine Basin; AM: Armorican Massif; AP: Armorican Platform; AR: Atlantic realm; CM: Central Massif; CP: Central Platform; LBM: London Brabant Massif; OP: Oriental Platform; PP: Provencal Platform; SB: Subalpine Basin; SOB: Souabe Basin.

measured on bulk carbonates (Umbria–Marche Basin: central Italy, Bartolini et al., 1996 and Bartolini and Cecca, 1999; Betic Cordillera: southern Spain, O'Dogherty et al., 2006 and Sandoval et al., 2008; Lusitanian Basin: Portugal, Suchéras-Marx et al., 2012; Subalpine Basin: southeast France, Suchéras-Marx et al., 2013) while oxygen isotope ratios have been measured in fish-tooth apatite (Paris Basin: northern France, Lécuyer et al., 2003; Luxemburg, Dera et al., 2009). Fossil-derived $\delta^{18}O$ data are, however, sparse for the Middle Jurassic of the western Tethys. We present new carbon and oxygen isotope data measured in well-preserved and biostratigraphically well-dated brachiopods selected from France (western Tethys).

For the first time, we made a compilation of published and new nannofossil data, which evidence the *Lotharingius–Watznaueria* turnover in the nannoplankton community through the Early–Middle Jurassic transition. We compared these data to newly-acquired and literature-derived carbon and oxygen isotope data. Correlating both datasets has allowed us to meaningfully discuss the paleoceanographic changes in terms of possible mechanisms (abiotic versus biotic) for triggering the *Lotharingius–Watznaueria* turnover.

2. Materials and methods

2.1. Compilation of nannofossil data

We compiled 860 semi-quantitative and quantitative abundances of *Lotharingius* and *Watznaueria* species from 28 sections, located in six different western Tethyan areas (central Italy; northern Italy and Switzerland; southeast France; southern Spain; western central Portugal; and southern Morocco; Fig. 1A). Among the 860 data, 274 are our own unpublished results from central Italy, Switzerland and Morocco (Fig. 1A). All the data have been calibrated with ammonite and/or ascribed to nannofossil zones (Subalpine Basin: southeast France, Erba, 1990; Lombardian Basin: northern Italy, Cobianchi et al., 1992; Umbria–Marche Basin: central Italy, Reale et al., 1992; Northern Apennines: northern Italy, Stoico and Baldanza, 1995; Ardèche: southeast France, Fauconnier et al., 1996; Lombardian Basin: Italy, Chiari et al., 2007; Betic Cordillera: southern Spain, Sandoval et al., 2008; Subalpine Basin: southeast France, Tiraboschi and Erba, 2010, Suchéras-Marx et al., 2015; Lusitanian Basin: western central Portugal, Suchéras-Marx et al., 2015). Then, we recalculated all the sample ages using the Geological Time Scale (GST 2012) of Gradstein et al. (2012), where the ammonite and nannofossil zones are correlated to absolute ages.

The main differences between the genera *Lotharingius* and *Watznaueria* concern the general arrangement of the shield and have been explained in Mattioli (1996). In the genus *Lotharingius*, the suture lines among the elements of the distal shield outer cycle appear less inclined than in the genus *Watznaueria*; under the light microscope, this produces an extinction pattern with isogyres showing an angle less than 90° between the bent arms for *Lotharingius*, and a right angle between the bent arms for *Watznaueria*. The general shape of *Watznaueria* coccoliths is marked concavo-convex, and cross structures can be also present in the central area of species of this genus, as in *Lotharingius*.

Watznaueria appeared at the end of the Early Toarcian, represented by the species *Watznaueria fossacincta* and *Watznaueria colacicchi* (Mattioli and Erba, 1999), although the major diversification occurred between the end of the Late Aalenian and the Early Bajocian, with the successive appearances of *Watznaueria britannica*, *Watznaueria*

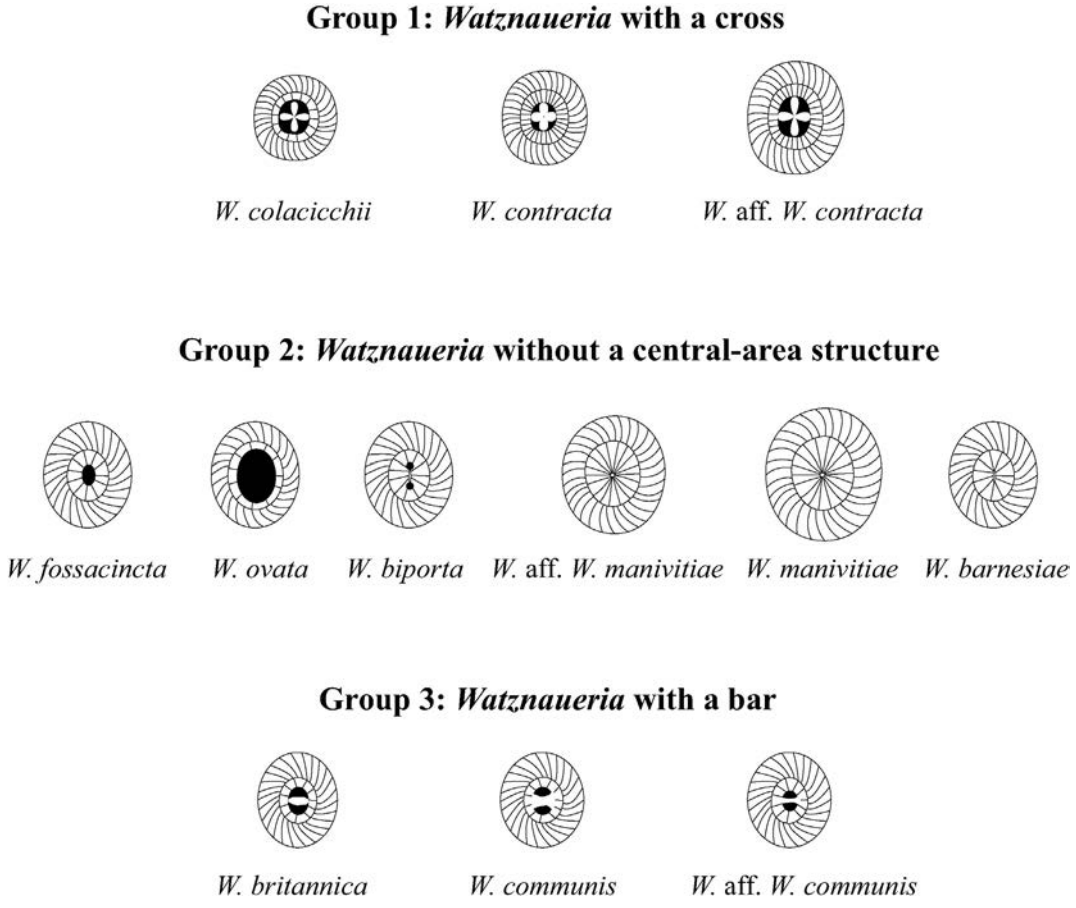

Fig. 2. Drawings of the main *Watznaueria* species belonging to the three morphological groups considered in this work. These groups were defined on the basis of presence/absence and type of central-area structure (cross, empty/closed, or bar).

communis, *Watznaueria* aff. *W. contracta*, *Watznaueria* aff. *W. manivitiae*, and *W. manivitiae* (Cobianchi et al., 1992). The appearances of *W.* aff. *W. communis* and *Watznaueria barnesiae* occurred later in the Late Bajocian and at the base of the Bathonian, respectively (see synthesis in Tiraboschi and Erba, 2010). In order to better understand the broader pattern of emergence and radiation of *Watznaueria* in terms of abundance, this genus was subdivided into three morphological groups, following the criteria described in Cobianchi et al. (1992) and refined in Mattioli (1996) and Mattioli and Erba (1999) (Fig. 2). The first group corresponds to *Watznaueria* with a cross in the central-area (*W. colacicchi*, *W. contracta*, *W.* aff. *W. contracta*), the second one to *Watznaueria* with no central-area structure (*W. barnesiae*, *Watznaueria biporta*, *W. fossacincta*, *W.* aff. *W. manivitiae*, *W. manivitiae*, *Watznaueria ovata*), and the third one to *Watznaueria* with a bar (*W. britannica*, *W. communis*, *W.* aff. *W. communis*). We carefully checked identifications in the different papers selected for this compilation, i.e. using both pictures and descriptions of *Watznaueria* species made by the authors, in order to be sure that our morphogroup criteria (cross, bar, closed or empty central-area) can be applied to produce a meaningful dataset.

Lotharingius species are lumped together here because the diversification of this genus is confined to the Early Jurassic, with no new species appearing in the Middle Jurassic (Mattioli and Erba, 1999; Fraguas and Young, 2011).

Semi-quantitative data are available from distribution charts in the literature, plotted as species abundance categories. Each category represents the abundance of each species in terms of specimens per field of view (FOV), estimated over 100 FOV in a slide under light-transmitting microscope at 1250× magnification, using a logarithmic-like scale (Bown and Young, 1998); all the papers we used for the compilation used the same logarithmic-like scale (e.g., Erba, 1990, Tiraboschi and Erba, 2010). These different categories are: A: abundant (more than 1 specimen per FOV); C: common (1 specimen in 1–9 FOV); F/C: few to common (1 specimen every 10 FOV); F: few (1 specimen in 11–29 FOV); R/F: rare to few (1 specimen every 30 FOV); R: rare (1 specimen in 31–100 FOV); VR: very rare (less than 1 specimen in 100 FOV); B: barren (not observed in the FOV). For each category, we divided the number of specimens by the average number of FOV in which they were recorded. Numerical values calculated for the different categories are: A > 1; C: 0.22 (average number of FOV: 4.5); F/C: 0.1; F: 0.05 (average number of FOV: 20); R/F: 0.033; R: 0.015 (average number of FOV: 65.5); VR: <0.01. Then the abundance numerical values of each group of species were clustered. This transformation allowed the assignment of a numerical value to semi-quantitative data for each morphological group in each sample. Nannofossil dataset compilation is reported in the Supplementary material.

2.2. Geochemistry

Thirty-nine fossil samples of brachiopod shells were selected from nine Middle Jurassic (uppermost part of the Late Toarcian to the Bajocian/Bathonian boundary) sections located in the southeastern part of the Paris Basin and in the Subalpine Basin (France). The samples are distributed across 5° of latitude (Fig. 1B). Stable carbon and oxygen isotope ratios were measured on the calcite of the secondary fibrous layer extracted from the adult part of the shells (Table 1).

Brachiopod shells selected for this study come from the 'Collections de Géologie de Lyon', seven of them having already been analyzed by Picard (2001, unpublished); they belong to the articulate group of rhynchonellids characterized by non-punctuate shells. Studied specimens have been biostratigraphically calibrated and are ascribed to well-constrained paleoenvironments (Table 1 and Fig. 1B). The paleoenvironments of brachiopods selected for this study range from the upper offshore to distal carbonate shelf or ramp. The upper offshore or mid-ramp lies between fair weather wave base and storm wave base (Reading, 1996). The distal carbonate ramp or outer ramp zone extends from below normal storm wave base to the pycnocline (Reading, 1996). Many outer- to mid-ramp environments are located within the photic zone, and are dominated by suspension feeders such as brachiopods and bivalves (Reading, 1996). Since brachiopods lived in the photic zone, we can consider that brachiopod-derived $\delta^{18}O$ data reflect changes in sea-surface temperatures.

Prior to isotopic analysis of the brachiopod shells, the samples were cleaned. The first step in the cleaning protocol is a mechanical removal of clays and of the primary layer of shell with a scraper under a binocular microscope. The primary layer of shell calcite was removed because it is not secreted in equilibrium with the ambient water (Carpenter and Lohmann, 1995; Auclair et al., 2003). Then samples were sonicated in double-deionized water. According to modern brachiopod studies, the calcite fibers of the secondary layer are precipitated in equilibrium with the surrounding waters and, the oxygen isotope composition should reflect local environmental conditions (Lowenstam, 1961; Veizer et al., 1986; Popp et al., 1986; Carpenter and Lohmann, 1995; Brand et al., 2003). However, as specialized portions of the secondary layer (e.g., brachidium, hinge, interarea, foramen, muscle scar) and the outermost part of the secondary layer are significantly ^{13}C- and ^{18}O-depleted, relative to expected equilibrium values (Carpenter and Lohmann, 1995; Auclair et al., 2003), they were not used for isotopic analysis. Finally, the powder of the remaining secondary fibrous layer of both ventral and dorsal valves was carefully extracted for isotopic analysis and was placed in clean vials.

The degree of preservation of the brachiopod shells was carefully assessed using scanning electron microscopy (SEM), in order to detect potential bias due to diagenetic overprinting of the primary isotopic signals. The shell microstructures are considered well-preserved when smooth fibrous surfaces of the secondary layer, very similar to recent specimens, are observed (Suan et al., 2008). Diagenetically-altered structures of the secondary layer of brachiopod shells are assessed when calcite fibers are poorly individualized (Suan et al., 2008). The pristine character of brachiopod shells, and especially the integrity of their stable isotope record, has also been tested by measuring the content of some key trace-elements, such as strontium, manganese and iron. In fact, some relationships between those trace-element contents and stable isotope ratios of marine invertebrate shells have been shown to be reliable indicators of the presence or absence of a diagenetic alteration of the studied fossils (Brand and Veizer, 1980; Veizer, 1983; Popp et al., 1986; Bruhn et al., 1995). Sr and Mn concentrations in about 5 mg of powdered brachiopod calcite samples were measured by ICP–MS, using the masses ^{88}Sr and ^{55}Mn. Indium was used as an internal standard. Distilled HNO_3 (4.5 M) was used for the digestion of these calcium carbonate shells. Overall reproducibility is estimated at $\pm 2\%$ (1σ) for these Sr and Mn measurements.

One to eight brachiopod specimens from the same species and from the same stratigraphic level were studied, in order to check for possible intra-specific isotopic differences. The calcite $\delta^{18}O$ and $\delta^{13}C$ values were determined in triplicate for every specimen using a MultiPrep™ automated preparation system, coupled to a dual-inlet Elementar Isoprime™ isotope-ratio mass spectrometer (IRMS) at the Laboratoire de Géologie de Lyon (UMR 5276, Université Claude Bernard Lyon 1). About 300 μg of brachiopod calcium carbonate were automatically reacted with anhydrous supersaturated phosphoric acid at 90 °C for 20 min, according to the method developed by Swart et al. (1991). Reproducibility of measurements was 0.1‰ (1σ) for $\delta^{18}O$ and 0.05‰ (1σ) for $\delta^{13}C$. Data are reported as $\delta^{18}O$ and $\delta^{13}C$ values vs. V-PDB (in ‰ δ units), after calibration with the NIST NBS-19 international standard, according to the protocol given by Werner and Brand (2001).

Table 1
Carbon and oxygen isotope ratios, and trace elements measured in brachiopod shells. Water temperatures calculated after the equation of Sharp (2007). For comparison are also given temperatures calculated using the oxygen isotope fractionation determined for synthetic calcite (Kim and O'Neil, 1997). Average seawater $\delta^{18}O$ value is assumed to be equal to −1‰ (V-SMOW) for an ice cap-free Jurassic world. Ammonite zones are from Alméras (1966, 1979a,b, 1996, 1997), Alméras and Elmi (1996) and Picard (2001, unpublished). Depositional settings of the selected localities are compiled from different papers (Rousselle, 1997; Ciszak et al., 2000; Picard, 2001, unpublished; Thiry-Bastien, 2002).

Brachiopod species	Sample no.	Université Lyon 1 — collection number	Age		Locality		Basin	Depositional environment	Sr (ppm)	Mn (ppm)	$\delta^{13}C_{carb}$ (‰ V-PDB)	$\delta^{18}O_{carb}$ (‰ V-PDB)	T seawater (°C) Kim and O'Neil (1997) inorganic calcite	T seawater (°C) Sharp (2007)
			Stage	Ammonite zone and subzone	Section	Area								
Data from this study														
Rhynchonelloidea ruthenensis	LeCom Rru1a	FSL 49229 (specimen no. 2)	Late Toarcian–Early Aalenian	Aalensis to Opalinum	Le Combalou (level 4)	Roquefort sur Soulzon (Aveyron)	SE	Homoclinal distal carbonate ramp	1311	43	1.416	−2.83	22.436	23.078
	LeCom Rru1b	FSL 49229 (specimen no. 4)							1106	39	1.809	−2.37	20.220	20.945
	LeCom Rru1c	FSL 49229 (specimen no. 8)							1060	27	2.036	−2.51	20.891	21.589
	LeCom Rru1d	FSL 49229 (specimen no. 17)							1134	34	2.470	−2.76	22.097	22.750
Rhynchonelloidea ruthenensis	LeCom Rru 2a	FSL 49230 (specimen no. 1)	Late Toarcian–Early Aalenian	Aalensis to Opalinum	Le Combalou (level 4)	Roquefort sur Soulzon (Aveyron)	SE	Homoclinal distal carbonate ramp	1057	53	1.787	−2.98	23.166	23.784
	LeCom Rru 2b	FSL 49230 (specimen no. 2)							1150	27	1.908	−2.28	19.791	20.534
	LeCom Rru 2c	FSL 49230 (specimen no. 3)							1067	38	2.271	−2.61	21.372	22.052
	LeCom Rru 2d	FSL 49230 (specimen no. 4)							995	27	1.675	−2.76	22.097	22.750
Rhynchonelloidea ruthenensis	LeCom Rru 3a	FSL 49236 (specimen no. 9)	Late Toarcian–Early Aalenian	Aalensis to Opalinum	Le Combalou (level 3)	Roquefort sur Soulzon (Aveyron)	SE	Homoclinal distal carbonate ramp	1102	23	1.509	−2.18	19.315	20.079
	LeCom Rru 3b	FSL 49236 (specimen no. 5)							1126	23	2.196	−2.44	20.555	21.267
	LeCom Rru 3c	FSL 49236 (specimen no. 29)							1315	28	2.033	−2.5	20.843	21.543
Rhynchonelloidea ruthenensis	LeCom Rru 4a	FSL 49259 (specimen no. 17)	Early Aalenian	Opalinum	Le Combalou (level 2)	Roquefort sur Soulzon (Aveyron)	SE	Homoclinal distal carbonate ramp	1183	25	2.296	−2.06	18.746	19.537
	LeCom Rru 4b	FSL 49259 (specimen no. 14)							1147	19	2.176	−2.6	21.324	22.005
	LeCom Rru 4c	FSL 49259 (specimen no. 28)							1247	14	2.548	−2.47	20.699	21.405
Rhynchonelloidea ruthenensis	LeCom Rru 5a	FSL 49264 (specimen no. 31)	Early Aalenian	Opalinum	Le Combalou (level 1)	Roquefort sur Soulzon (Aveyron)	SE	Homoclinal distal carbonate ramp	1060	34	2.285	−2.21	19.458	20.215
	LeCom Rru 5b	FSL 49264 (specimen no. 36)							1065	22	2.1	−1.95	18.227	19.043
	LeCom Rru 5c	FSL 49264 (specimen no. 44)							1030	20	2.557	−2.45	20.603	21.313
	LeCom Rru 5d	FSL 49264 (specimen no. 55)							1090	27	2.174	−2.41	20.412	21.129
Rhynchonelloidea ruthenensis	Tourm Rru1a	FSL 49272 (specimen no. 12)	Early Aalenian	Opalinum	Tournemire	Aveyron	SE	Homoclinal distal	1105	24	2.339	−1.9	17.991	18.819

								carbonate ramp						
	Tourm Rru1b	FSL 49272 (specimen no. 22)							1065	34	2.431	−2.28	19.791	20.534
	Tourm Rru1c	FSL 49272 (specimen no. 28)							1043	25	2.385	−2.25	19.648	20.397
	Tourm Rru1d	FSL 49272 (specimen no. 29)							1004	27	2.593	−2.12	19.030	19.808
Globirhynchia subobsoleta	Belmo Gsu1a	FSL 307796 (specimen no. 1)	Early Aalenian	Opalinum (Comptum subzone)	Belmont	Rhône	SE	Very distal shelf with deep currents	1022	17	1.766	−1.14	14.460	15.492
Globirhynchia subobsoleta	Belmo Gsu2a	FSL 307795 (specimen no. 1)	Middle Aalenian	Murchisonae (Haugi subzone)	Belmont	Rhône	SE	Distal shelf with tempestites			2.475	−0.98	13.728	14.810
	Belmo Gsu2b	FSL 307795 (specimen no. 2)							936	15	2.424	−1.03	13.956	15.022
Rhynchonelloidea subangulata	Culev Rsu1a	FSL 49282 (specimen no. 30)	Middle Aalenian–Early Bajocian	Murchisonae to Laeviuscula	Coulevon	Haute-Saône	Paris	Upper offshore	1232	57	2.294	−0.6	12.004	13.213
Rhynchonelloidea subangulata	Comb Rsu1a	FSL 49289 (specimen no. 43)	Middle Aalenian–Early Bajocian	Murchisonae to Laeviuscula	Comberjon	Haute-Saône	Paris	Upper offshore	1170	26	2.160	−1.15	14.506	15.535
Lacunaerhynchia vergissonensis	Ronze Lve1a	FSL 45717 (specimen no. 1)	Early Bajocian	Humphriesianum	Roncevaux	Davayé (Saône et Loire)	Paris	Upper offshore	1055	8	2.383	−0.95	13.591	14.683
Caucasella voultensis	PoEto Cvo1a	FSL 308222 (specimen no. 1)	Late Bajocian/Early Bathonian boundary		Pont des Etoiles	Rompon (Ardèche)	SE	Mass flow deposits from shallow water facies with hydraulic accumulations	512	73	2.304	−0.98	13.728	14.810
	PoEto Cvo1b	FSL 308222 (specimen no. 2)							482	30	2.033	−0.68	12.365	13.546
	PoEto Cvo1c	FSL 308222 (specimen no. 3)							505	23	2.289	−0.72	12.546	13.714
	PoEto Cvo1d	FSL 308222 (specimen no. 4)							447	72	2.175	−0.85	13.136	14.260
Data from Picard (2001)														
Rhynchonella angulata	Coul		Early Bajocian	Discites to Propinquans	Coulevon	Haute-Saône	Paris	Upper offshore			2.2	−2.7	21.807	22.470
Cymatorhynchia sp.	13-Solutré		Early Bajocian	Humphriesianum	Solutré	Saône et Loire	Paris	Upper offshore			1.9	−2	18.463	19.267
Rhynchonella	Cour. 1		Early Bathonian	Zigzag (Convergens subzone)	Courlon	Côte d'Or	Paris	Upper offshore			1.2	−0.7	12.456	13.630
Rhynchonella	Cour. 1*		Early Bathonian	Zigzag (Convergens subzone)	Courlon	Côte d'Or	Paris	Upper offshore			1.2	−0.8	12.909	14.049
Rhynchonella	Cour. 2		Early Bathonian	Zigzag (Convergens subzone)	Courlon	Côte d'Or	Paris	Upper offshore			1.7	−2.5	20.843	21.543
Rhynchonella	Cour. 2*		Early Bathonian	Zigzag (Convergens subzone)	Courlon	Côte d'Or	Paris	Upper offshore			1.5	−2.6	21.324	22.005
Rhynchonella voultensis	Vob		Middle to Late Bathonian	Bremeri to Discus	La Voulte	Ardèche	SE	Distal upper offshore			2.1	−0.3	10.658	11.977

The $\delta^{18}O$ of biogenic calcite is linked, by a thermodynamic effect, to the isotopic composition ($\delta^{18}O_w$) and temperature of the seawater (Urey, 1947) in which calcification took place (Duplessy et al., 1991). $\delta^{18}O$ of the biogenic carbonate is temperature-dependent and can be converted into a water temperature value knowing or assuming the $\delta^{18}O_w$ of ambient water. Since the pioneering studies published by Epstein et al. (1953) and Craig (1965), several oxygen-isotope fractionation equations for biogenic calcite have been proposed (e.g. Anderson and Arthur, 1983; Bemis et al., 1998; Sharp, 2007). They resulted from successive refinements in the knowledge of isotopic fractionations involved during sample preparation, i.e. equilibration between CO_2 and H_2O and acid digestion of carbonates; these data are critical in performing conversions between the SMOW and PDB scales. In addition, there is a sizable effect of Mg content on oxygen isotope fractionation between calcite and water (Tarutani et al., 1969; Jiménez-López et al., 2004) that was estimated to increase at a rate of 0.06 to 0.17 per mol% of $MgCO_3$, (Jiménez-López et al., 2004; Brand et al., 2013). Calcite of studied brachiopods contains no more than 3 mol% of $MgCO_3$ as estimated from literature data and Raman spectroscopy, which means that uncertainties in estimates of paleotemperatures could reach up to 2 °C. In this study, emphasis is placed on relative variations in water temperature through time, rather than on absolute temperatures.

Self-consistency with the V-SMOW scale, and the latest refined data concerning knowledge of the acid fractionation factor taking place during the acid digestion of calcite, led Sharp (2007) to propose a new isotopic fractionation equation. Water temperature is related to the $\delta^{18}O$ of calcite and water as follows:

$$T(°C) = 15.75 - 4.3 * (\delta^{18}O_{carb} - \delta^{18}O_{water}) + 0.12 * (\delta^{18}O_{carb} - \delta^{18}O_{water})^2.$$

This equation was used in this study to estimate marine paleotemperatures. It is worthy to note that calculated temperatures are close to those obtained by using the oxygen isotope fractionation determined for synthetic calcite (Table 1) precipitated in the laboratory by Kim and O'Neil (1997). In the framework of our study, $\delta^{18}O_{water}$ is assumed to be equal to −1‰ for ice-cap-free periods (Shackleton and Kennett, 1975), as it is commonly assessed for most of the Jurassic (Picard et al., 1998; Lécuyer et al., 2003; Rosales et al., 2004; Dera et al., 2009; Suan et al., 2008, 2010).

3. Results

3.1. Changes through time of Lotharingius and Watznaueria abundances

Fig. 3 shows the variation through time of the abundances of the three morphogroups of *Watznaueria* and of *Lotharingius*. *Lotharingius* species were dominant from the Late Toarcian through the Aalenian, whereas low abundances are recorded in the Late Bajocian–Bathonian interval. This group shows a long-term decreasing trend during the studied interval with a small rebound located around the Aalenian/Bajocian boundary. *Watznaueria* with a cross shows a large abundance peak at the Aalenian/Bajocian boundary. *Watznaueria* without central-area structures increases from the base of Bajocian upwards. *Watznaueria* with a bar sharply increases from the base of Bajocian upwards. Both increases in abundance of *Watznaueria* without central-area structure, and *Watznaueria* with a bar occurred a short time after the large peak in *Watznaueria* with a cross, and also correspond to the new entry of various species of this genus in the Early Bajocian and at the Bajocian/Bathonian boundary, as already recognized in *Watznaueria* phyletic trees (Cobianchi et al., 1992; Erba, 1990; Mattioli and Erba, 1999; Tiraboschi and Erba, 2010). The peak of *Watznaueria* with a cross observed at the Aalenian/Bajocian boundary is described here for the first time.

3.2. Geochemistry

SEM analyses revealed the generally good state of preservation of the brachiopod secondary fibrous structures, which are smooth and well-individualized (Fig. 4). Sr (447 to 1315 ppm) and Mn (8 to 73 ppm) contents of Jurassic brachiopod shells (Table 1) compare well with those of unaltered recent brachiopod shells in which Sr and Mn range from 800 to 2200 ppm and 10 to 50 ppm, respectively (Morrison and Brand, 1986). The four analyzed samples from Ardèche (France) are characterized by the lowest Sr contents (~500 ppm), whereas all the other samples have Sr contents ranging from 936 to 1315 ppm (Fig. 5). It is worth noting that these Ardèche brachiopods show among the highest $\delta^{18}O$ values, despite their low Sr content.

Carbon isotope ratios of the fibrous secondary layer range from 1.20 to 2.59‰ (V-PDB), while oxygen isotope ratios comprised between −2.98 and −0.30‰ (V-PDB) (Table 1). There is no correlation between these two variables, considering either the whole sample collection or data clusters defined on the basis of the various sampled sites (Fig. 5).

In summary, the microstructures of the brachiopod shells, as revealed by SEM observation as well as trace elemental content, indicate that the studied brachiopods have not, or only weakly, been altered by secondary diagenesis.

The trends in carbon and oxygen isotope data are shown in Fig. 6A and B. Despite large intraspecific variations (around 1‰), the $\delta^{13}C$ values slightly increase from the latest Toarcian (mean value of 1.9‰) to the earliest Aalenian (mean value of 2.4‰, *Leioceras opalinum* Ammonite Zone; Fig. 6A). The lowest $\delta^{13}C$ value is recorded in the earliest Bathonian (1.2‰).

Intraspecific variations (around 1‰) are also identified in the $\delta^{18}O$ record, but the stratigraphic trend presents larger variations through time, compared to the $\delta^{13}C$ record. Mean $\delta^{18}O$ values increase from the latest Toarcian (−2.6‰) to the Middle Aalenian (−0.94‰; Fig. 6B); only one $\delta^{18}O$ value obtained from a different species is higher than the surrounding ones (−1.1‰; Fig. 6B). From the Middle Aalenian to the Early Bathonian, $\delta^{18}O$ values are comparable. The highest value of −0.3‰ is recorded in the Late Bathonian (Fig. 6B).

3.3. Evolution of the $\delta^{13}C$ record and $\delta^{18}O$-derived temperatures across the Aalenian–Bathonian interval

In order to better determine the Middle Jurassic $\delta^{13}C$ and temperature trends (based on the oxygen isotope record), brachiopod carbon isotope ratios and $\delta^{18}O$-derived temperatures were associated with data obtained from other brachiopods (Paris Basin, Brigaud et al., 2009), belemnites (Lusitanian Basin, Jenkyns et al., 2002; Paris Basin, Dera et al., 2009; Basque–Cantabrian Basin, Gomez et al., 2009; see compilations in Dera et al., 2011), and fish (Paris Basin, Lécuyer et al., 2003; Dera et al., 2009). Carbon isotope ratios measured on bulk carbonates (Umbria–Marche Basin, Bartolini et al., 1996 and Bartolini and Cecca, 1999; Betic Cordillera, O'Dogherty et al., 2006; Sandoval et al., 2008; Lusitanian Basin, Suchéras-Marx et al., 2012; Subalpine Basin, Suchéras-Marx et al., 2013) have also been reported. All the available isotope data have been gathered and smoothed to extract long-term trends (Fig. 7A and B).

For the $\delta^{13}C$ record, the most remarkable trend is a pronounced positive excursion in the Early Bajocian within a long-term stable trend from the latest Toarcian until the end of the Bathonian (Fig. 7A). The 1‰ offset observed for the $\delta^{13}C_{bulk\ carbonate}$ in the Aalenian (Fig. 7A) corresponds to the differences recorded between the Umbria–Marche and Betic Cordillera basins (Sandoval et al., 2008). The more negative $\delta^{13}C$ values are recorded by belemnites for the Late Aalenian (Fig. 7A); however belemnites have a larger

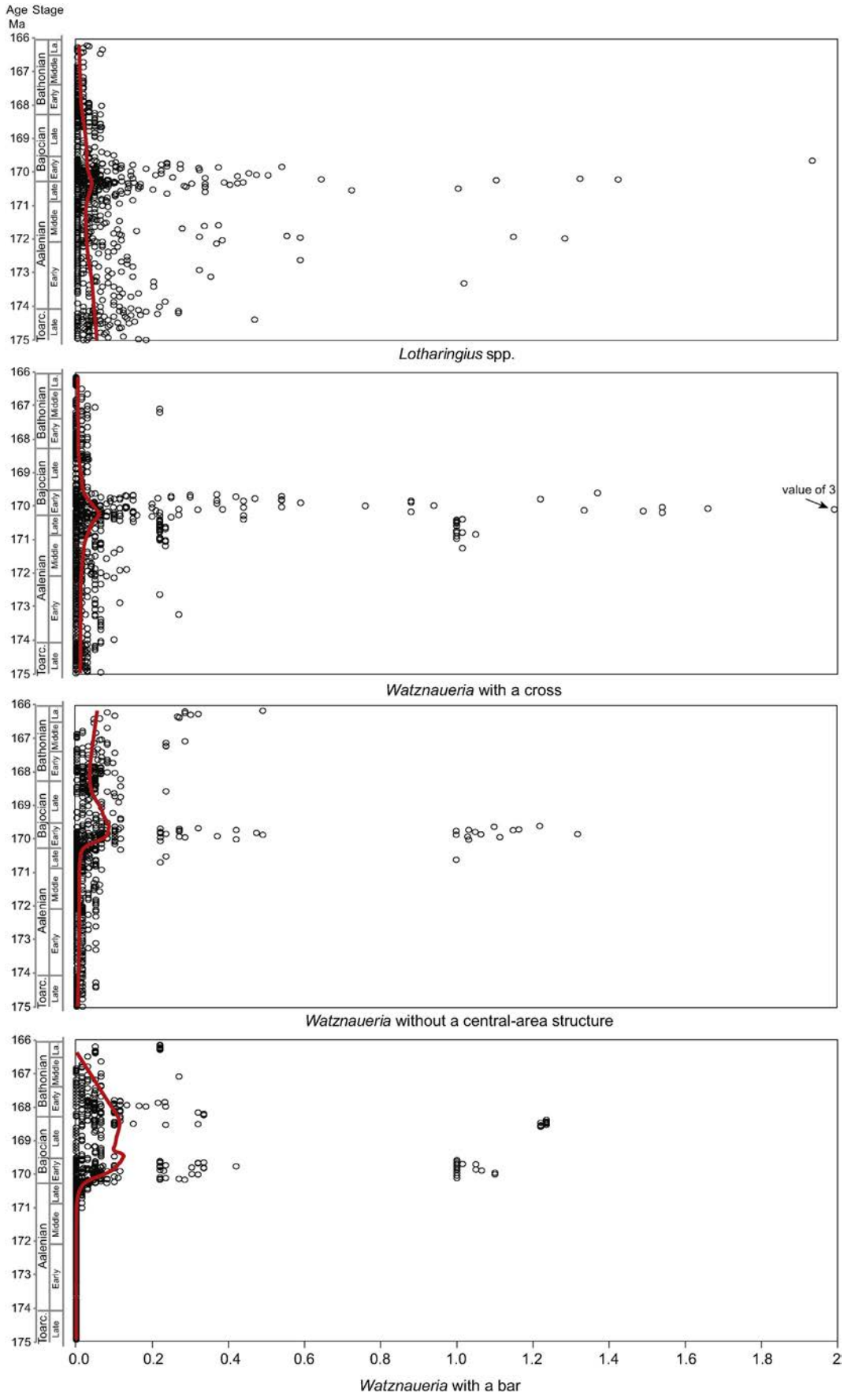
Age Stage
Ma
Bathonian
Bajocian
Aalenian
Toarc.
Middle
Early
Late
166
167
168
169
170
171
172
173
174
175
Lotharingius spp.
value of 3
Watznaueria with a cross
Watznaueria without a central-area structure
0.0
0.2
0.4
0.6
0.8
1.0
1.2
1.4
1.6
1.8
2
Watznaueria with a bar

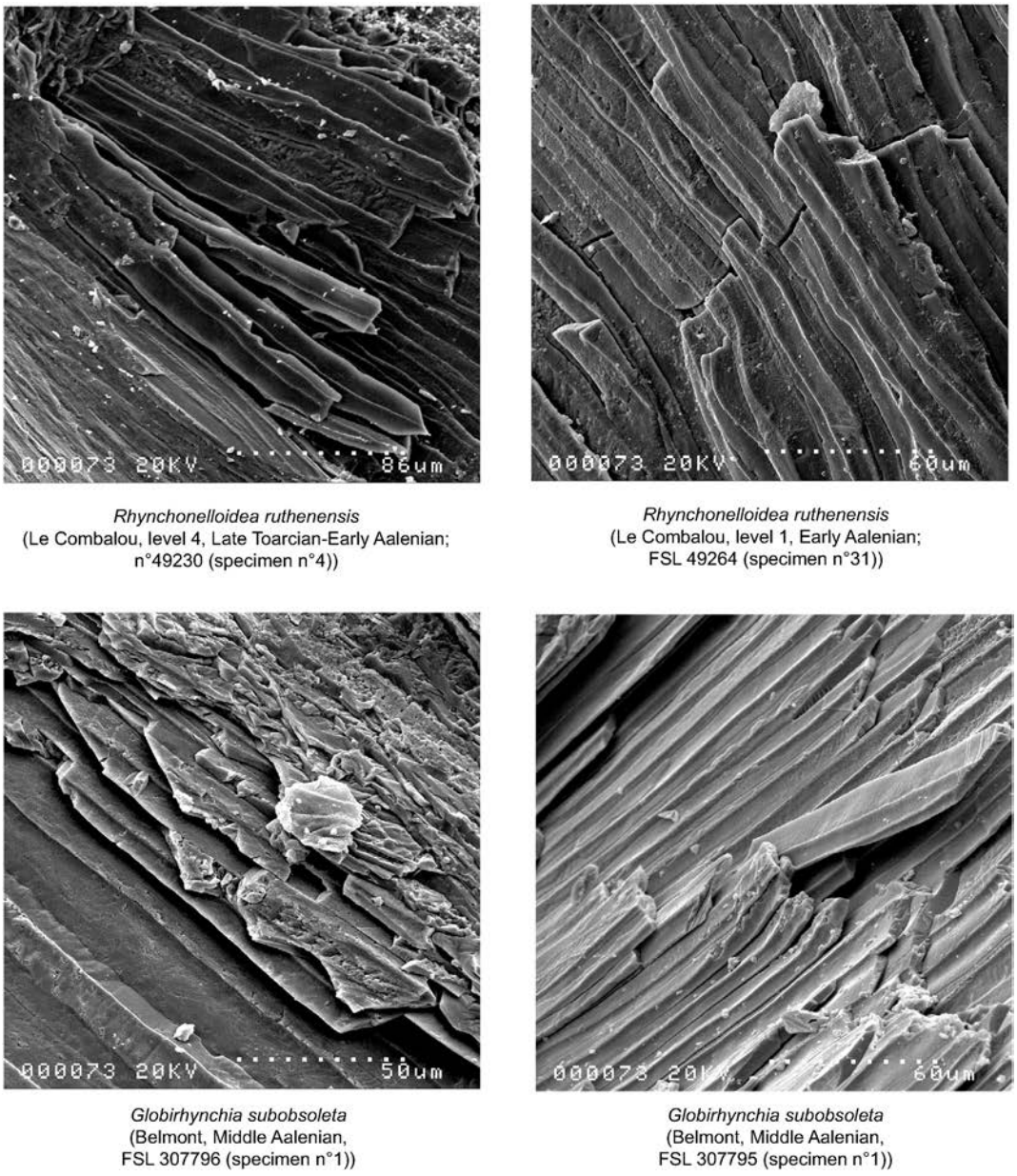

Rhynchonelloidea ruthenensis
(Le Combalou, level 4, Late Toarcian-Early Aalenian;
n°49230 (specimen n°4))

Rhynchonelloidea ruthenensis
(Le Combalou, level 1, Early Aalenian;
FSL 49264 (specimen n°31))

Globirhynchia subobsoleta
(Belmont, Middle Aalenian,
FSL 307796 (specimen n°1))

Globirhynchia subobsoleta
(Belmont, Middle Aalenian,
FSL 307795 (specimen n°1))

Fig. 4. SEM micrographs of selected rhynchonellid specimens analyzed in this work. See Table 1 for more information on the specimen numbers.

range of $\delta^{13}C$ values (−1.3 to 4.5‰) than both brachiopods and bivalves, as well as bulk rocks (Fig. 7A).

A long-term cooling trend is apparent from the uppermost Toarcian (mean value of 22 °C) to the earliest Bajocian (mean value of 14 °C; Fig. 7B). A short-lived (less than 1 Myr) significant recovery of about 4 °C took place in the late Early Bajocian (mean value of 18 °C), followed by a second cooler period in the Late Bajocian (mean values around 16 °C; Fig. 7B). Despite a large dispersion of the values in the Late Bathonian, a warming trend is observed (Fig. 7B).

4. Discussion

Diagenetic re-equilibration of the chemical composition of a marine calcium carbonate may occur through a mechanism of dissolution–precipitation involving waters of meteoric origin. In this framework,

Fig. 3. Compilation of transformed semi-quantitative abundances (860 samples from 28 sections located in six different western Tethyan basins) for *Lotharingius* lumped and the three morphological groups of *Watznaueria*, as defined in this study. Numerical values along the bottom correspond to the abundance numerical values of each group of species: *Watznaueria* with a cross, *Watznaueria* with a bar, other *Watznaueria* (without a structure in the central-area), and *Lotharingius* spp. (see text, Section 2.1 for explanations, and Supplementary material). A LOESS (LOcal regrESSion) smoothing was applied to the data, in order to better appreciate the general trend, by using PAST (Hammer et al., 2001). The LOESS smoothing is a method combining the multiple least-square regression model in a nearest neighbor model. The LOESS depends on n, the number of points, and q, the degree of smoothing (from 0 to 1 in PAST). The program fits the nq points around each given point to a straight line (least-square regression), with a weighing function decreasing with distance. Each n straight line generated is then connected to form the LOESS curve (in red). With increasing a q value, the smoothing incorporates a higher number of n points. The degree of smoothing applied to the database is 0.3.

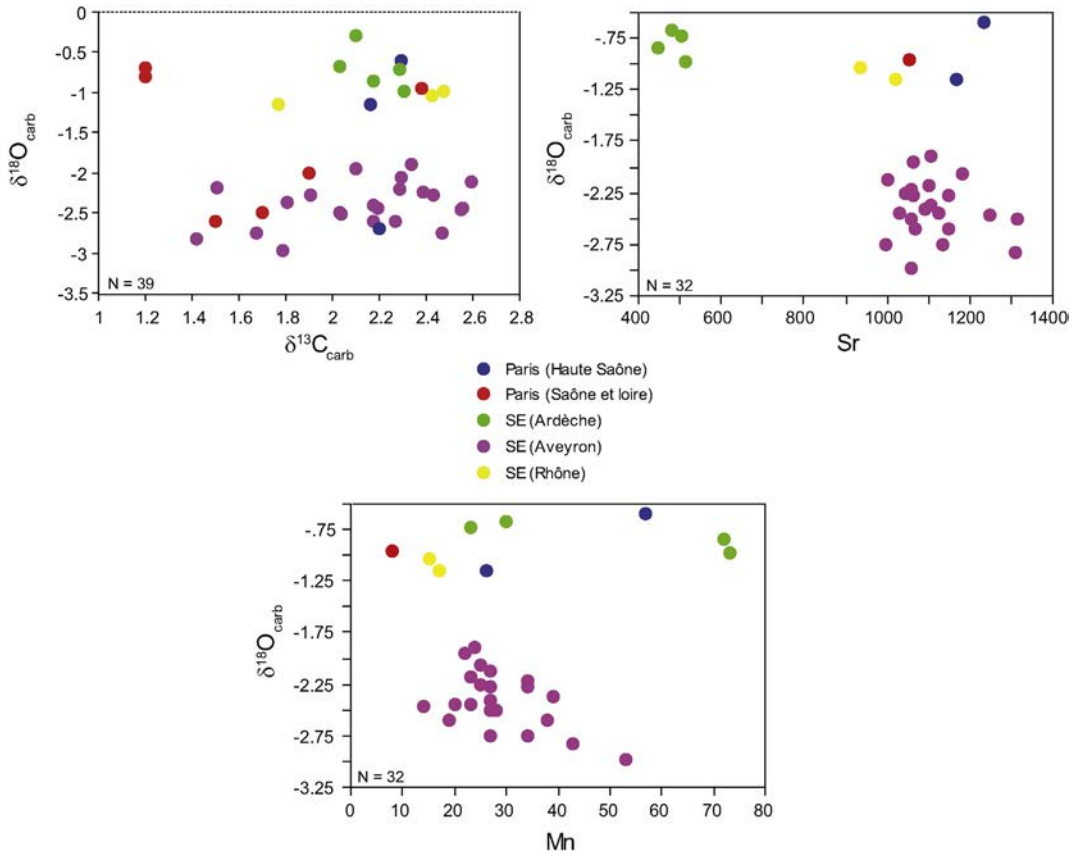

Fig. 5. Bivariate plots showing the relationship between $\delta^{18}O$ and $\delta^{13}C$, Sr, Mn values of the brachiopods. Colored dots represent the different French localities. N = number of measured specimens. Trace elements were not measured in brachiopods analyzed by Picard (2001, unpublished).

thermodynamics predict that recrystallized shells must be Sr-depleted and Mn-enriched, relative to their pristine chemical compositions (Brand and Veizer, 1980; Veizer, 1983). Therefore, any record of the progress of the water–carbonate chemical reaction must be illustrated by a positive correlation between the $\delta^{18}O$ values and Sr concentrations of the brachiopod shells, while a negative correlation is expected between $\delta^{18}O$ and Mn concentrations. Such correlations are not observed in our data, considering either the entire collection of samples, or data by location (Fig. 5). Moreover, the trace element contents of the studied brachiopod shells fall in the same ranges as those that were documented for modern unaltered brachiopods, suggesting the absence of addition to, or loss from, the shell calcite. It is also emphasized here that there is no correlation between $\delta^{13}C$ and $\delta^{18}O$ values reinforcing the idea of a negligible effect of diagenesis on these brachiopod samples. Indeed, a positive correlation between these two isotope ratios could indicate water–carbonate reactions that took place after the death and burial of these marine organisms (e.g. Jenkyns and Clayton, 1986).

The coccolith semi-quantitative abundance record, along with the smoothed $\delta^{13}C$ and $\delta^{18}O$ records, are reported in Fig. 8. Most of the Middle Jurassic (except the Callovian, not studied here) seems to be a stable interval until significant biotic and paleoenvironmental changes occurred during the Late Aalenian–Early Bajocian.

The Aalenian–Bajocian transition records a turnover from assemblages dominated by *Lotharingius* spp. to assemblages dominated by *Watznaueria* without a central-area structure and *Watznaueria* with a bar. This turnover coincides with the peak of *Watznaueria* with a cross. Thus, this peak marks a turning point in terms of paleoenvironmental changes. An increase in calcareous nannofossil flux, and consequently in pelagic carbonate production, both in the Mediterranean and Submediterranean Tethys successions of the Lusitanian and Subalpine basins has been identified (Suchéras-Marx et al., 2014). Benthic foraminifera, which inhabited the Basque–Cantabrian Basin in northern Spain and the Lusitanian Basin in western Portugal, underwent major extinctions in the latest Aalenian (Canales, 2001; Gomez et al., 2009; Canales and Henriques, 2013). In the latter area, the disappearance of typical Early Jurassic brachiopods is also recorded just below the Aalenian/Bajocian boundary (Andrade, 2004). The peak of *Watznaueria* with a cross also coincides with the onset of a gradual decrease in seawater $^{87}Sr/^{86}Sr$ (Jenkyns et al., 2002; Wierzbowski et al., 2012), reflecting a major input of mantle-derived Sr by hydrothermal fluids linked to increasing mid-ocean ridge activity.

In the Early Bajocian (*Hyperlioceras discites* and *Witchellia laeviuscula* ammonite zones), the abundance increases in both *Watznaueria* without a central-area structure and *Watznaueria* with a bar correspond to a major diversification of the *Watznaueria* genus lasting for about 1.5 Myr (Suchéras-Marx et al., 2013, 2014, 2015), and was associated with diversification or radiations of other marine planktic (radiolarians; Bartolini et al., 1999), nektonic (ammonoids; O'Dogherty et al., 2006) and benthic (foraminifera, brachiopods; Andrade, 2004; Vörös, 2005; Canales and Henriques, 2013) groups. At that time, typical Middle Jurassic forms in the different fossil groups first appeared and replaced Lower Jurassic assemblages. These biotic changes are concomitant with the onset of a positive carbon isotope excursion spanning the entire Early Bajocian (Suchéras-Marx et al., 2013), and corresponding to the lowest recorded temperatures (Fig. 8). The Lower Bajocian positive $\delta^{13}C$ excursion has been related to an increasing productivity in sea-surface waters (Bartolini et al., 1996, 1999), as attested by a rise in biogenic silica production and deposits,

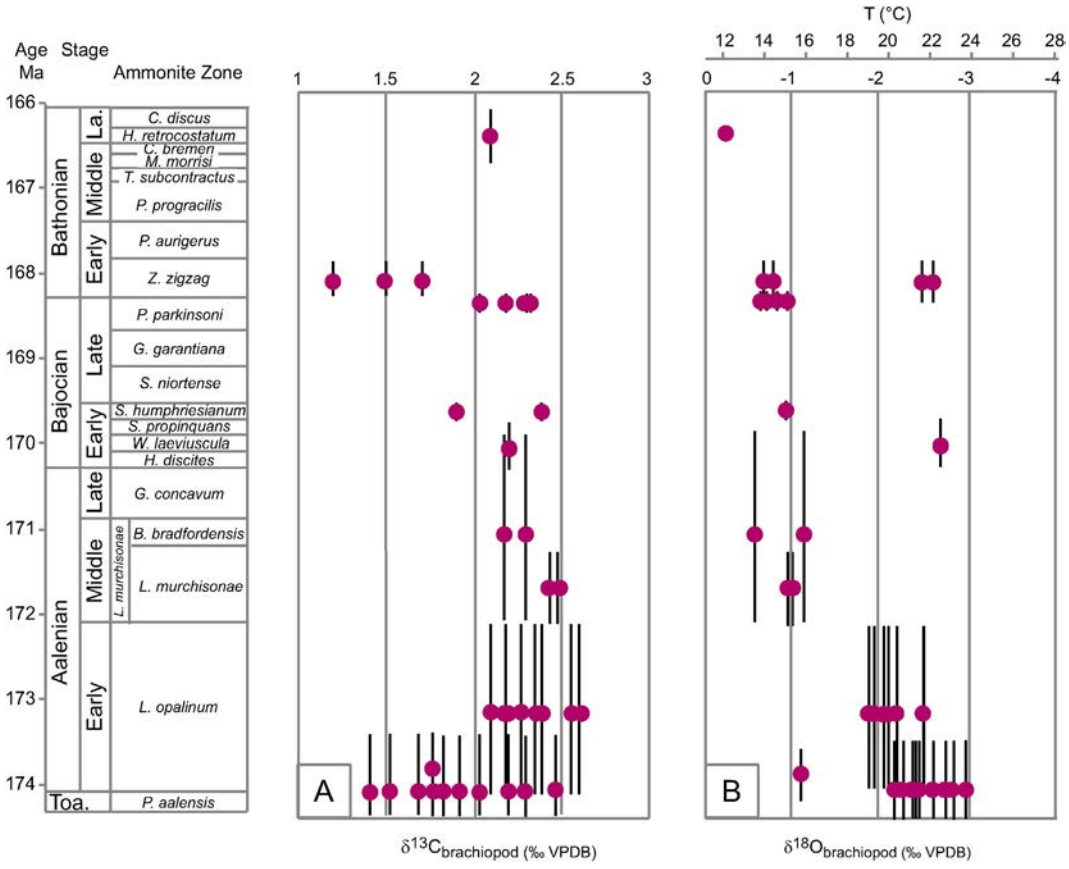

Fig. 6. A. Carbon isotope ratios measured on brachiopod calcite (this work). B. Oxygen isotope ratios measured on brachiopod calcite (this work); error bars represent the age uncertainty. Numerical ages correspond to GTS2012 (Gradstein et al., 2012) and the ammonite zonation is from the Groupe Français d'Études du Jurassique (1997).

both in neritic and pelagic environments of various basins located in the western Tethys (Bartolini et al., 1996, 1999; Bill et al., 2001; Cobianchi, 2002; Chiari et al., 2007; Gorican et al., 2012).

The onset of ocean opening, as attested by the decreasing $^{87}Sr/^{86}Sr$ ratio (Jenkyns et al., 2002; Wierzbowski et al., 2012), potentially triggered a rearrangement of oceanic circulation. During the Middle Jurassic, deep-water connections between the Alpine ocean and the eastern part of the western Tethys have been inferred by Baumgartner (1987) and Bill et al. (2001), on the basis of the distribution of radiolarites in the Tethyan ophiolites. Moreover, westward, the onset of a mid-latitude, circum-global circulation, linked to the widening of the Hispanic Corridor, could have promoted upwelling at tropical latitudes (Hotinski and Toggweiler, 2003). Cool seawater temperatures (this study; Dera et al., 2011) concomitant with positive shifts in εNd(t), are also interpreted as possible evidence of Tethyan upwelling development (Dera et al., 2014). The occurrence of upwelling in this oceanographic context could explain the increase in marine surface water fertility, as suggested by our data compilation.

An increase in continental weathering, and in the associated nutrients supplied to the ocean, constitutes another explanation for the higher primary production assumed for the Early Bajocian. More humid conditions, deduced from the presence of coal–charcoal deposits in England (Hesselbo et al., 2003), as well as from clay mineralogical assemblages described from France and Hungary (Raucsik et al., 2001; Raucsik and Varga, 2008; Brigaud et al., 2009), have been suggested for the Early Bajocian. Combined paleoceanographic and climatic changes could have been responsible for an increase in the productivity of sea surface waters that eventually triggered faunal radiations. The end of the turnover is characterized by a short-lived temperature increase. Following this interval, paleoenvironmental conditions seem to have become stable again.

Watznaueria seems therefore very sensitive to paleoceanographic and paleoclimatic changes across the Aalenian–Bajocian. In particular, specimens with a cross in the central area seem to be opportunistic form, proliferating in times of water-mass instability related to nutrients and temperature. The eventual radiation of *Watznaueria* with a bar and with a closed central area in the Early Bajocian marks the beginning of a long-term dominance of the genus in coccolith assemblages that lasted through the rest of the Jurassic. *Watznaueria* overcame the most profound environmental changes of the Cretaceous (i.e., oceanic anoxic events) and has proved to be one of the most eurytopic taxa of the Mesozoic (Cobianchi, 2002; Lees et al., 2005; Mutterlose et al., 2005).

5. Conclusions

A compilation of abundance changes of *Lotharingius* and *Watznaueria*, which were the successive dominant taxa in coccolith assemblages of the Early–Middle Jurassic, has been made for the first time. A comparison of this significant overturn in the coccolith community with the $\delta^{13}C$ record and $\delta^{18}O$-derived temperatures has led us to identify likely forcing through major paleoceanographic and climatic events that took place during a short interval around the Aalenian–Bajocian transition.

In the coccoliths, a turnover from assemblages dominated by *Lotharingius* to assemblages dominated by *Watznaueria* without a

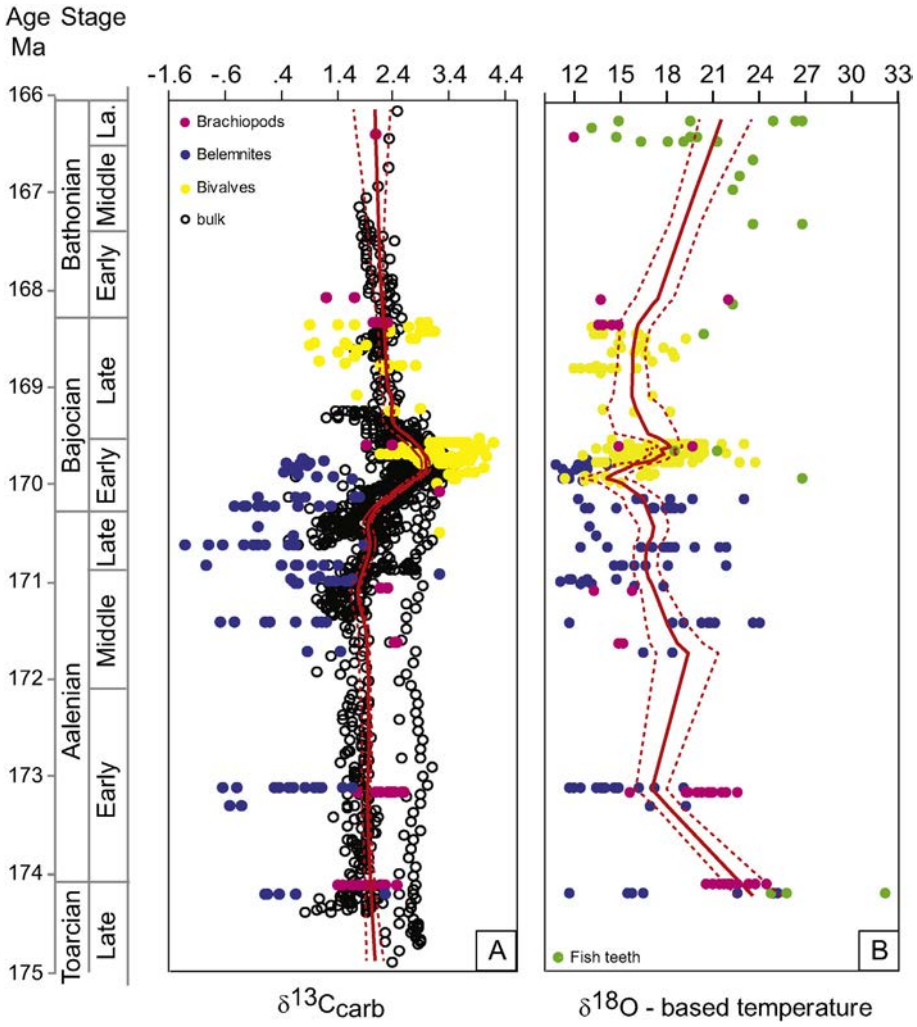

Fig. 7. A. Carbon isotope data from this study (brachiopods) and from the literature (belemnites, bivalves, and bulk) compiled and smoothed. A LOESS smoothing was applied to the data in order to better appreciate the general trend by using PAST (Hammer et al., 2001). The degree of smoothing was set to 0.2 (red line). B. Temperature data from this study (brachiopods) and from literature (belemnites, bivalves, and fish) compiled, similarly to the $\delta^{13}C$ record.

central-area structure and *Watznaueria* with a bar is recorded across the Aalenian/Bajocian boundary. This turnover coincides with a substantial abundance peak of *Watznaueria* with a cross, which has been identified here for the first time. *Watznaueria* with a cross proliferated during a transient period characterized by the opening of large oceanic domains, such as the Alpine Tethys and the Central Atlantic, along with a rearrangement of the oceanic circulation that favored the development of some pioneering taxa in the nannoplankton community, but also triggered extinctions in several marine groups. An opportunistic behavior is thus inferred for *Watznaueria* with a cross.

As a second step, the major diversification of *Watznaueria*, and the dominance of *Watznaueria* with a structureless central-area took place in the Early Bajocian associated with radiations in other marine groups. These biotic changes occurred during a time of enhanced oceanic fertility and relatively low marine temperatures.

This study suggests that evolution, diversification and dominance in the coccolithophorid community was favored during a short turnover interval (around 1.5 Myr), when major paleoceanographic changes took place. This interval separates long-term, stable times, when the dominance of a particular group could become well-established, such as *Lotharingius* during the Toarcian–Aalenian and *Watznaueria* with no central-area structure for the Bajocian–Bathonian and later.

Acknowledgments

We are grateful to the Editor Frans Jorissen, Jackie Lees and an anonymous reviewer for both English corrections and comments which greatly improved the quality of an earlier version of the manuscript. This study was supported by the projects BQR 2006 of the Université Lyon 1 to FG, BQR 2010 and INSU 2011 Syster/Interrvie to EM. The Laboratories UMR 5275 at the University Grenoble 1 and UMR 5276 at the University Lyon 1 are also acknowledged. This study was supported by a post-doctoral grant of the CNRS/INSU (Centre National de la Recherche Scientifique/Institut National des Sciences de l'Univers) to G.E. López-Otálvaro. Brachiopod specimens used in this study for geochemical analyses are cured in the Collections de Géologie de l'Université de Lyon; collection numbers are indicated in Table 1 (FSL number).

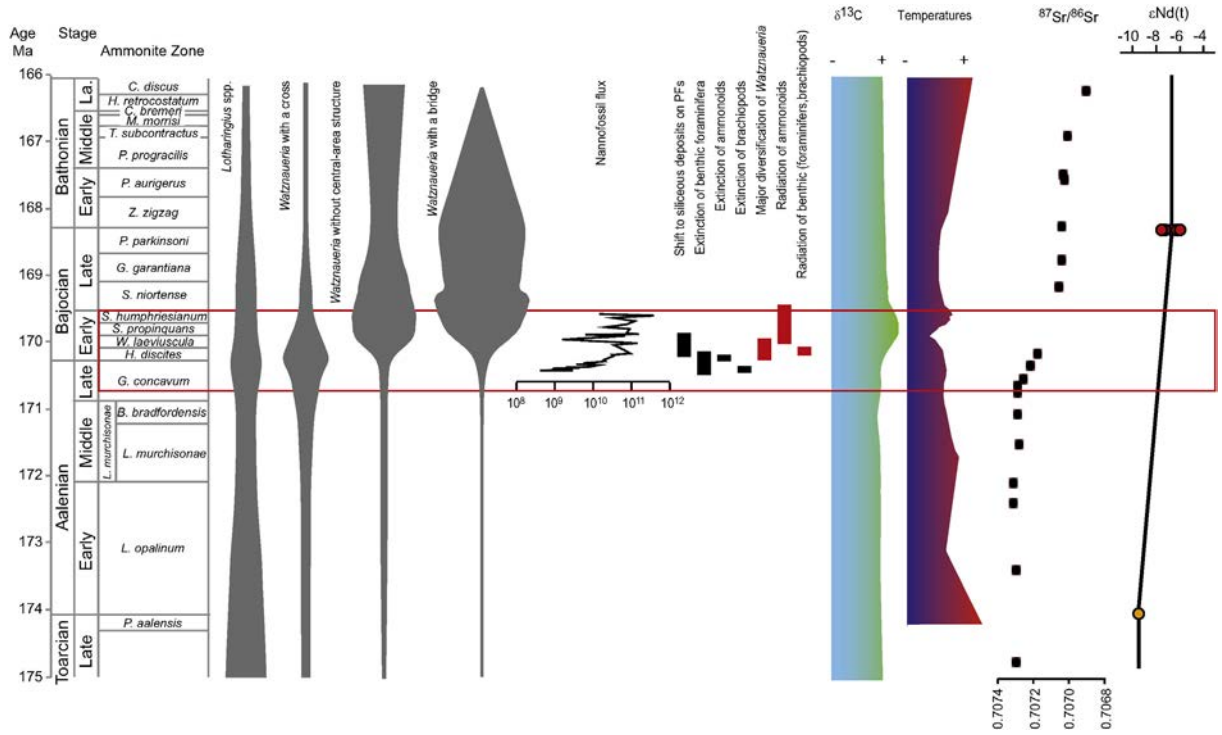

Fig. 8. Long-term smoothed changes in the *Lotharingius–Watznaueria*, with respect to external paleoenvironmental data, namely the $\delta^{13}C$ record and calculated marine temperatures inferred from the $\delta^{18}O$ record based on brachiopods, bivalves and fish teeth, and $^{87}Sr/^{86}Sr$ and $\varepsilon Nd(t)$ from the latest Toarcian (Toa.) to the Late Bathonian. Nannofossil flux data from Suchéras-Marx et al. (2013). The compilation of biotic change is based on several publications (Bartolini et al., 1996, 1999; Bill et al., 2001; Leindfelder et al., 2002; Andrade, 2004; Vörös, 2005; O'Dogherty et al., 2006; Chiari et al., 2007; Léonide et al., 2007; Gomez et al., 2009; Gorican et al., 2012; Canales and Henriques, 2013). $^{87}Sr/^{86}Sr$ ratios are from Jenkyns et al. (2002; Toarcian–Bajocian), and Wierzbowski et al. (2012; Bathonian), and the $\varepsilon Nd(t)$ is from Dera et al. (2014); A focus is made on the Aalenian–Bajocian transition where major biotic and abiotic changes are recorded.

Appendix A. Supplementary data

Supplementary data to this article can be found online at http://dx.doi.org/10.1016/j.marmicro.2016.03.001.

References

Alméras, Y., 1966. Les Rhynchonellidés du Bajocien moyen de Ronzevaux, près Davayé (Saône-et-Loire): genres *Cymatorhynchia* BUCKMAN, *Lacunaerhynchia* nov. Et *Septulirhynchia* nov. Trav. Lab. Géol. Fac. Sci. Lyon N. S. 13, 31–119.

Alméras, Y., 1979a. Etude morphologique et anatomique de *Rhynchonelloidea ruthenensis* (REYNES). Justification de la distinction des genres *Homoeorhynchia* BUCKMAN et *Rhynchonelloidea* BUCKMAN (Brachiopoda). Geobios 12 (2), 187–221.

Alméras, Y., 1979b. Etude morphologique et anatomique de *Rhynchonelloidea subangulata* (DAV.) (Brachiopoda, Rhynchonelloidae). Doc. Lab. Géol. Lyon. 76, 3–21.

Alméras, Y., 1996. Les Brachiopodes toarciens et aaléniens inférieurs du Bassin du Rhône. Paléontologie et biostratigraphie. Révisions de la collection Dumortier et compléments. Doc. Lab. Géol. Lyon. 138, 1–123.

Alméras, Y., 1997. The genus *Caucasella* MOISSEEV (Brachiopoda, Rhynchonellacea) in the Middle Jurassic of the French North-Tethyan Realm. Boll. Soc. Paleontol. Ital. 35 (3), 257–276.

Alméras, Y., Elmi, S., 1996. Le genre *Cymatorhynchia* Buckman (Brachiopoda, Rhynchonellacea) dans le Bajocien–Bathonien de la bordure vivaro-cévenole (Bassin du Sud-Est, France). Cadre stratigraphique et paléogéographique. Beringeria 18, 201–245.

Anderson, T.F., Arthur, M.A., 1983. Stable isotopes of oxygen and carbon and their application to sedimentologic and paleonvironmental problems. In: Arthur, M.A., Anderson, T.F., Kaplan, I.R., Veizer, J., Land, L.S. (Eds.), Stable Isotopes in Sedimentary Geology. SEPM Short Course, No.10, pp. 1–151.

Andrade, J.B., 2004. Los Braquiopodos del Transito Jurasico Inferior–Jurasico Medio de la Cuenca Lusitanica (Portugal) Ph.D. Thesis Universidad Complutense de Madrid, Madrid (251 p).

Auclair, A.-C., Joachimski, M.M., Lécuyer, C., 2003. Deciphering kinetic, metabolic and environmental controls on stable isotope fractionations between seawater and the shell of *Terebratalia transversa* (Brachiopoda). Chem. Geol. 202, 59–78.

Balch, W.M., 2004. Re-evaluation of the physiological ecology of coccolithophores. In: Thierstein, H.R., Young, J.R. (Eds.), Coccolithophores, From Molecular Processes to Global Impact. Springer-Verlag, Berlin Heidelberg, pp. 165–190.

Bartolini, A., Cecca, F., 1999. 20 My hiatus in the Jurassic of Umbria–Marche Apennines (Italy): carbonate crisis due to eutrophication. CR Acad. Sci. Paris 329, 587–595.

Bartolini, A., Baumgartner, P.O., Hunziker, J.C., 1996. Middle and Late Jurassic carbon stable-isotope stratigraphy and radiolarite sedimentation of the Umbria–Marche Basin (Central Italy). Eclogae Geol. Helv. 89, 811–844.

Bartolini, A., Baumgartner, P.O., Guex, J., 1999. Middle and Late Jurassic radiolarian palaeoecology versus carbon-isotope stratigraphy. Palaeogeogr. Palaeoclimatol. Palaeoecol. 145 (1–3), 43–60.

Baumgartner, P.O., 1987. Age and genesis of Tethyan Jurassic radiolarites. Eclogae Geol. Helv. 80, 831–879.

Bemis, B.E., Spero, H.J., Bijma, J., Lea, D.W., 1998. Reevaluation of the oxygen isotopic composition of planktonic foraminifera: experimental results and revised paleotemperature equations. Paleoceanography 13, 150–160.

Bill, M., O'Dogherty, L., Guex, J., Baumgartner, P.O., Masson, H., 2001. Radiolarite ages in Alpine–Mediterranean ophiolites: constraints of the continental breakup and the Tethys–Atlantic connection. Geol. Soc. Am. Bull. 113 (1), 129–143.

Bown, P.R., 1987. Taxonomy, evolution, and biostratigraphy of the late Triassic–early Jurassic calcareous nannofossils. Special Papers in Paleontology. The Palaeontological Association, London (118 p).

Bown, P.R., Young, J.R., 1998. Techniques. In: Bown, P.R. (Ed.), Calcareous Nannofossil Biostratigraphy. Chapman and Hall (Kluwer Academic Publishers), Dordrecht, pp. 2–28.

Brand, U., Veizer, J., 1980. Chemical diagenesis of a multi-component carbonate system — 1: trace elements. J. Sediment. Petrol. 50, 1219–1236.

Brand, U., Logan, A., Hiller, N., Richardson, J., 2003. Geochemistry of modern brachiopods: applications and implications for oceanography and paleoceanography. Chem. Geol. 198, 305–334.

Brand, U., Azmy, K., Bitner, M.A., Logan, A., Zuschin, M., Came, R., Ruggiero, E., 2013. Oxygen isotopes and $MgCO_3$ in brachiopod calcite and a new paleotemperature equation. Chem. Geol. 359, 23–31.

Brigaud, B., Durlet, C., Deconinck, J.-F., Vincent, B., Pucéat, E., Thierry, J., Trouiller, A., 2009. Facies and climate/environmental changes recorded on a carbonate ramp: a sedimentological and geochemical approach on Middle Jurassic carbonates (Paris Basin, France). Sediment. Geol. 222 (3–4), 181–206.

Bruhn, F., Bruckschen, P., Richter, D.K., Meijer, Stephan, A., Veizer, J., 1995. Diagenetic history of sedimentary carbonates: constraints from combined cathodoluminescence and trace element analyses by micro-PIXE. Nucl. Instrum. Methods Phys. Res. Sect. B 104, 409–414.

Canales, M.L., 2001. Los foraminíferos del Aaleniense (Jurasico Medio) en la Cuenca Vasco-Cantabrica (N de Espana). Rev. Esp. Micropaleontol. 33, 253–438.

Canales, M.L., Henriques, M.H., 2013. Foraminiferal assemblages from the Bajocian Global Stratotype Section and Point (GSSP) at Cabo Mondego. J. Foraminifer. Res. 43, 182–206.

Carpenter, S.J., Lohmann, K.C., 1995. $\delta^{18}O$ and $\delta^{13}C$ values of modern brachiopod shells. Geochim. Cosmochim. Acta 59, 3749–3764.

Chiari, M., Cobianchi, M., Picotti, V., 2007. Integrated stratigraphy (radiolarians and calcareous nannofossils) of Middle to Upper Jurassic Alpine radiolarites (Lombardian Basin, Italy): constraints to their genetic interpretation. Palaeogeogr. Palaeoclimatol. Palaeoecol. 249, 233–270.

Ciszak, R., Peybernes, B., Fauré, P., Thierry, J., 2000. Géométrie et enchaînement des séquences de dépôt aaléno-bajociennes dans les Grands Causses (France). Strata 10, 61–63.

Cobianchi, M., 1992. Sinemurian–Early Bajocian calcareous nannofossil biostratigraphy of the Lombardy Basin (southern Calcareous Alps; Northern Italy). Atti Ticin. Sci. Terra 35, 61–106.

Cobianchi, M., 2002. Calcareous nannofossils from the Middle and Upper Jurassic of the Belluno Basin (Southern Calcareous Alps). AttiTicinensi di Scienze della Terra 43, 2–24.

Cobianchi, M., Erba, E., Pirini-Radrizzani, C., 1992. Evolutionary trends of calcareous nannofossil genera *Lotharingius* and *Watznaueria* during the Early and Middle Jurassic. Sci. Geol. Mem. Padova 43, 19–25.

Craig, H., 1965. The measurement of oxygen isotope paleotemperatures. In: Tongiorgi, E. (Ed.), Stable Isotopes in Oceanographic Studies and Paleotemperatures. Laboratorio di Geologia Nucleare, Pisa, pp. 161–182.

Dera, G., Pucéat, E., Pellenard, P., Neige, P., Delsate, D., Joachimski, M.M., Reisberg, L., Martinez, M., 2009. Water mass exchange and variations in seawater temperature in the NW Tethys during the Early Jurassic: evidence from neodymium and oxygen isotopes of fish teeth and belemnites. Earth Planet. Sci. Lett. 286, 198–207. http://dx.doi.org/10.1016/j.epsl.2009.06.027.

Dera, G., Brigaud, B., Monna, F., Laffont, R., Puceat, E., Deconinck, J.-F., Pellenard, P., Joachimski, M.M., Durlet, C., 2011. Climatic ups and downs in a disturbed Jurassic world. Geology 39, 215–218.

Dera, G., Prunier, J., Smith, P.L., Haggart, J.W., Popov, E., Guzhov, A., Rogovf, M., Delsate, D., Thies, D., Cuny, G., Pucéat, E., Charbonnier, G., Bayon, G., 2014. Nd isotope constraints on ocean circulation, paleoclimate, and continental drainage during the Jurassic breakup of Pangea. Gondwana Res. http://dx.doi.org/10.1016/j.gr.2014.02.006.

Duplessy, J.-C., Labeyrie, L., Juillet–Leclerc, A., Maître, F., Duprat, J., Sarnthein, M., 1991. Surface salinity reconstruction of the North Atlantic Ocean during the last glacial maximum. Oceanol. Acta 14, 311–324.

Enay, R., Mangold, C., 1980. Synthèse paléogéographique du Jurassique Français par Le Groupe français d'Etude du Jurassique Cariou E., Contini D., Debrand-Passard S., Donze P., Gabilly J., Lefavrais-Raymond A., Mouterde R., Thierry J. (coord). Docum. Lab. Géol. Lyon H.S. 5, 210 p. 1 fig., 3 tabl., 42 cartes.

Epstein, S., Buchsbaum, R., Lowenstam, H.A., Urey, H.C., 1953. Revised carbonate–water isotopic temperature scale. Geol. Soc. Am. Bull. 64, 1315–1326.

Erba, E., 1990. Calcareous nannofossil biostratigraphy of some Bajocian sections from the Digne area (SE France). Memorie Descrittive Della Carta Geologica d'Italia Vol. XL, pp. 237–256.

Fauconnier, D., Courtinat, B., Gardin, S., Lachkar, G., Rauscher, R., 1996. Biostratigraphy of Triassic and Jurassic series in the borehole "Balazuc1" (GPF program). Stratigraphy context inferred from spores, pollens, dinoflagellates cysts and nannofossils. Mar. Pet. Geol. 13, 707–724.

Fraguas, A., Young, J.R., 2011. Evolution of the coccolith genus *Lotharingius* during the Late Pliensbachian–Early Toarcian interval in Asturias (N Spain). Consequences of the Early Toarcian environmental perturbations. Geobios 44, 361–375.

Gomez, J.J., Canales, M.L., Ureta, S., Goy, A., 2009. Palaeoclimatic and biotic changes during the Aalenian (Middle Jurassic) at the southern Laurasian Seaway (Basque–Cantabrian Basin, northern Spain). Palaeogeogr. Palaeoclimatol. Palaeoecol. 275, 14–27.

Gorican, S., Pavsic, J., Rozic, B., 2012. Bajocian to Tithonian age of radiolarian cherts in the Tolmin Basin (NW Slovenia). Bull. Soc. Geol. Fr. 183 (4), 369–382.

Gradstein, F.M., Ogg, J.G., Schmitz, M.D., Ogg, G.M., 2012. The Geologic Time Scale 2012. Vol. 2. Elsevier, Amsterdam.

Groupe français du Jurassique (coordinated by Cariou, E., and P. Hantzpergue), 1997a. Biostratigraphie du Jurassique ouest-européen et méditerranéen: zonations parallèles et distribution des invertébrés et microfossiles. Bull. Centres Rech. Explor. Prod. Elf-Aquitaine Mémoire 17 (422 p).

Hammer, Ø., Harper, D.A.T., Ryan, P.D., 2001. PAST: paleontological statistics software package for education and data analysis. Palaeontol. Electron. 4 (1) (9 p).

Hesselbo, S.P., Morgans-Bell, H.S., McElwain, J.C., Rees, P.M., Robinson, S.A., Ross, C.E., 2003. Carbon-cycle perturbation in the middle Jurassic and accompanying changes in the terrestrial paleoenvironment. J. Geol. 111, 259–276.

Hotinski, R.M., Toggweiler, J.R., 2003. Impact of a Tethyan circumglobal passage on ocean heat transport and "equable" climates. Paleoceanography 18 (1), 1007. http://dx.doi.org/10.1029/2001PA000730.

Jenkyns, H.C., Clayton, C.J., 1986. Black shales and carbon isotopes in pelagic sediments from the Tethyan Lower Jurassic. Sedimentology 33, 87–106.

Jenkyns, H.C., Jones, C.E., Gröcke, D.R., Hesselbo, S.P., Parkinson, P.N., 2002. Chemostratigraphy of the Jurassic System: applications, limitations and implications for paleoceanography. J. Geol. Soc. Lond. 159, 351–378.

Jiménez-López, C., Romanek, C.S., Huertas, F.J., Ohmoto, H., Caballero, E., 2004. Oxygen isotope fractionation in synthetic magnesian calcite. Geochim. Cosmochim. Acta 68, 3367–3377.

Kim, S.-T., O'Neil, J.R., 1997. Equilibrium and nonequilibrium oxygen isotope effects in synthetic carbonates. Geochim. Cosmochim. Acta 61, 3461–3475.

Lécuyer, C., Picard, S., Garcia, J.P., Sheppard, S.M.F., Grandjean, P., Dromart, G., 2003. Thermal evolution of Tethyan surface waters during the Middle–Late Jurassic: evidence from $\delta^{18}O$ values of marine fish teeth. Paleoceanography 18, 1–16.

Lees, J.A., Bown, P.R., Mattioli, E., 2005. Problems with proxies? Cautionary tales of calcareous nannofossil paleoenvironmental indicators. Micropaleontology 51 (4), 333–343.

Leindfelder, R.R., Schimd, D.U., Nose, M., Wenrer, W., 2002. Jurassic reef patterns — the expression of a changing globe. In: Kiessling, W., Flügel, E., Golonka, J. (Eds.), Phanerozoic Reef Patterns. SEPM Vol. 72, pp. 465–520.

Léonide, P., Floquet, M., Villier, L., 2007. Interaction of tectonics, eustasy, climate and carbonate production on the sedimentary evolution of an early/middle Jurassic extensional basin (Southern Provence Sub-basin, SE France). Basin Res. 19, 125–152.

Linnert, C., Mutterlose, J., 2009. Evidence of increasing surface water oligotrophy during the Campanian–Maastrichtian boundary interval: calcareous nannofossils from DSDP Hole 390A (Blake Nose). Mar. Micropaleontol. 73, 26–36.

Lowenstam, H.A., 1961. Mineralogy, $^{18}O/^{16}O$ ratios, and strontium, and magnesium contents of recent and fossil brachiopods and their bearing on the history of the oceans. J. Geol. 69, 241–260.

Mattioli, E., 1996. New calcareous nannofossil species from the Early Jurassic of Tethys. Riv. Ital. Paleontol. Stratigr. 102, 397–412.

Mattioli, E., Erba, E., 1999. Synthesis of calcareous nannofossil events in Tethyan Lower and Middle Jurassic successions. Riv. Ital. Paleontol. Stratigr. 105, 343–376.

McIntyre, A., Bé, A.W.H., Roche, M.B., 1970. Modern Pacific coccolithophorida: a paleontological thermometer. N.Y. Acad. Sci. Trans. 32 (6), 720–731.

Morrison, J.O., Brand, U., 1986. Geochemistry of recent marine invertebrates. Geosci. Can. 13, 237–254.

Mutterlose, J., Bornemann, A., Herrle, J.O., 2005. Mesozoic calcareous nannofossils — state of the art. Paläontol. Z. 79, 113–133.

O'Dogherty, L., Sandoval, J., Bartolini, A., Bruchez, S., Bill, M., Guex, J., 2006. Carbon isotope stratigraphy and ammonite faunal turnover for the Middle Jurassic in the Southern Iberian palaeomargin. Palaeogeogr. Palaeoclimatol. Palaeoecol. 239 (3–4), 311–333.

Okada, H., Honjo, S., 1973. The distribution of ocean coccolithophorids in the Pacific. Deep-Sea Res. 20, 335–374.

Picard, S., 2001. Evolution des eaux ouest-téthysiennes (température, bathymétrie) au cours du Jurassique moyen à supérieur à partir des enregistrements géochimiques ($\delta^{18}O$, $\delta^{13}C$, Terres rares) de faunes marines. Unpublished PhD Thesis, University Claude Bernard Lyon 1, Lyon, 260 p.

Picard, S., Garcia, J.-P., Lécuyer, C., Sheppard, S.M.F., Cappetta, H., Emig, C.C., 1998. $\delta^{18}O$ values of coexisting brachiopods and fish: Temperature differences and estimates of paleo-water depths. Geology 26, 975–978.

Popp, B.N., Anderson, T.F., Sandberg, P.A., 1986. Brachiopods as indicators of original composition in some Paleozoic limestones. Geol. Soc. Am. Bull. 97, 1262–1269.

Raucsik, B., Varga, A., 2008. Climato-environmental controls on clay mineralogy of the Hettangian–Bajocian successions of the Mecsek Mountains, Hungary: an evidence for extreme continental weathering during the early Toarcian oceanic anoxic event. Palaeogeogr. Palaeoclimatol. Palaeoecol. 265 (1–2), 1–13.

Raucsik, B., Demény, A., Borbély-Kiss, I., Szabó, G., 2001. Monsoon-like climate during the Bajocian. Clay mineralogical and geochemical study on a limestone/marl alternation (Komló Calcareous Marl Formation, Mecsek Mountains, Southern Hungary). Hantkeniana 3, 149–176.

Reading, H.G., 1996. Sedimentary Environments: Processes, Facies and Stratigraphy. third ed. Blackwell Science (688 p).

Reale, V., Baldanza, A., Monechi, S., Mattioli, E., 1992. Calcareous nannofossil biostratigraphy events from the Early–Middle Jurassic sequences of Umbria–Marche area (Central Italy). Sci. Geol. Mem. 42, 41–75.

Rosales, I., Quesada, S., Robles, S., 2004. Paleotemperature variations of Early Jurassic seawater recorded in geochemical trends of belemnites from the Basque–Cantabrian Basin, northern Spain. Palaeogeogr. Palaeoclimatol. Palaeoecol. 203, 253–275.

Rousselle, B., 1997. Partition stratigraphique des faciès et des volumes de dépôt en domaine de plate-forme carbonatée: exemple dans l'Aalénien su Sud-Est de la France. Doc. Lab. Géol. Lyon 143 (225 p).

Sandoval, J., O'Dogherty, L., Aguado, R., Bartolini, A., Bruchez, S., Bill, M., 2008. Aalenian carbon-isotope stratigraphy: calibration with ammonite, radiolarian and nannofossil events in the Western Tethys. Palaeogeogr. Palaeoclimatol. Palaeoecol. 267, 115–137.

Shackleton, N.J., Kennett, J.P., 1975. Paleotemperature history of the Cenozoic and initiation of Antarctic glaciation: oxygen and carbon isotopic analyses in DSDP Sites 277, 279, and 281. In: Kennett, J.P., Houtz, R.E., et al. (Eds.), Initial Report of DSDP Vol. 29. U.S. Government Printing Office, Washington, pp. 743–755.

Sharp, Z.D., 2007. Principles of Stable Isotope Geochemistry. Pearson Prentice Hall, New Jersey (344 p).

Stoico, M., Baldanza, A., 1995. Early and Middle Jurassic calcareous nannofossil biozonation of the Monti Sabini area (Latium, Northern Apennines, Central Italy). Palaeopelagos 5, 75–110.

Suan, G., Mattioli, E., Pittet, B., Maillot, S., Lécuyer, C., 2008. Evidence for major environmental perturbation prior to and during the Toarcian (Early Jurassic) oceanic anoxic event from the Lusitanian Basin, Portugal. Paleoceanography 23, PA1202. http://dx.doi.org/10.1029/2007PA001459.

Suan, G., Mattioli, E., Pittet, B., Lécuyer, C., Suchéras-Marx, B., Duarte, L.V., Philippe, M., Reggiani, L., Martineau, F., 2010. Secular environmental precursors to early Toarcian (Jurassic) extreme climate changes. Earth Planet. Sci. Lett. 290, 448–458. http://dx.doi.org/10.1016/j.epsl.2009.12.047.

Suchéras-Marx, B., Guihou, A., Giraud, F., Lécuyer, C., Allemand, P., Pittet, B., Mattioli, E., 2012. Impact of the Middle Jurassic diversification of *Watznaueria* (coccolith-bearing algae) on the carbon cycle and ^{13}C of bulk marine carbonates. Glob. Planet. Chang. 86–87, 92–100.

Suchéras-Marx, B., Giraud, F., Fernandez, V., Pittet, B., Lécuyer, C., Olivero, D., Mattioli, E., 2013. Duration of the Early Bajocian and the associated $\delta^{13}C$ positive excursion based on cyclostratigraphy. J. Geol. Soc. Lond. 170, 107–118.

Suchéras-Marx, B., Giraud, F., Mattioli, E., Gally, Y., Barbarin, N., Beaufort, L., 2014. Middle Jurassic coccolith fluxes: a novel approach by automated quantification. Mar. Micropaleontol. 111, 15–25.

Suchéras-Marx, B., Giraud, F., Mattioli, E., Escarguel, G., 2015. Paleoenvironmental and paleobiological origins of coccolithophorid genus *Watznaueria* emergence during the Late Aalenian–Early Bajocian. Paleobiology 41, 415–435.

Swart, P.K., Burns, S.J., Leder, J.J., 1991. Fractionation of the stable isotopes of oxygen and carbon in carbon dioxide during the reaction of calcite with phosphoric acid as a function of temperature and technique. Chem. Geol. (Isotope Geoscience Section) 86, 89–96.

Tarutani, T., Clayton, R.N., Mayeda, T.K., 1969. The effect of polymorphism and magnesium substitution on oxygen isotope fractionation between calcium carbonate and water. Geochim. Cosmochim. Acta 33, 987–996.

Thiry-Bastien, P., 2002. Stratigraphie séquentielle des calcaires bajociens de l'Est de la France (Jura-Bassin de Paris). Unpublished thesis, Université Claude Bernard Lyon 1, 407 p.

Tiraboschi, D., Erba, E., 2010. Calcareous nannofossil biostratigraphy (Upper Bajocian–Lower Bathonian) of the Ravin du Bès section (Bas Auran, Subalpine Basin, SE France): evolutionary trends of *Watznaueria barnesiae* and new findings of "*Rucinolithus*" morphotypes. Geobios 43 (1), 59–76.

Urey, H.C., 1947. The thermodynamic properties of isotopic substances. J. Chem. Soc. 562–581.

Veizer, J., 1983. Trace elements and isotopes in sedimentary carbonates. Rev. Mineral. Geochem. 11, 265–299.

Veizer, J., Fritz, P., Jones, B., 1986. Geochemistry of brachiopods: oxygen and carbon isotopic records of Paleozoic oceans. Geochim. Cosmochim. Acta 50, 1679–1696.

Vörös, A., 2005. The smooth brachiopods of the Mediterranean Jurassic: refugees or invaders? Palaeogeogr. Palaeoclimatol. Palaeoecol. 223, 222–242.

Werner, R.A., Brand, W.A., 2001. Referencing strategies and techniques in stable isotope ratio analysis. Rapid Commun. Mass Spectrom. 15, 501–519.

Wierzbowski, H., Anczkiewicz, R., Bazarnik, J., Pawlak, J., 2012. Strontium isotope variations in Middle Jurassic (Late Bajocian–Callovian) seawater: implications for Earth's tectonic activity and marine environments. Chem. Geol. 334, 171–181. http://dx.doi.org/10.1016/j.chemgeo.2012.10.019.

Ziegler, P.A., 1988. Evolution of the Arctic–North Atlantic and the Western Tethys. Am. Assoc. Petr. Geol. Mem. 43, 164–196.